2008 IEEE/RSJ International Conference on Intelligent Robots and Systems
Acropolis Convention Center
Nice, France, Sept, 22-26, 2008

Autonomous Dynamic Balance of an Electrical Bicycle Using Variable Structure Under-Actuated Control

Chih-Lyang Hwang*, Hsiu-Ming Wu** and Ching-Long Shih**
* Department of Electrical Engineering, Tamkang University, Taipei County, Taiwan
** Department of Electrical Engineering, National Taiwan University of Science and Technology, Taipei, Taiwan

Abstract --- In an electric bicycle, two strategies are taken up to stabilize the running motion of a bicycle. One is the control of its center of gravity (CG), and the other is the control of its steering angle of handle. In general, the control of the CG is used a pendulum. In addition, the motion of a bicycle often possesses a lean angle with respect to vertical direction. In this situation, the proposed system contains three outputs: steering angle, lean angle, and pendulum angle, these will affect the dynamic balance of an electrical bicycle. The proposed control generating the handle torque and pendulum toque is called variable structure under-actuated control (VSUAC). The motivation of using the VSUAC is that the system uncertainties of a bicycle are often huge due to different ground conditions and a gust of wind. Merely use an ordinary proportional-derivative-integral (PID) control or other linear controls often can not have good robust performance. Finally, the compared simulations for the electrical bicycle among ordinary PID control, modified proportional-derivative control (MPDC), and VSUAC confirm the usefulness of our proposed control.

Index Terms: Electrical bicycle, Dynamic balance, Variable structure under-actuated control, Modified proportional-derivative control, Lyapunov stability.

I. Introduction

There are many papers on the stabilization control of the two-wheeled vehicle. In 1971, Sharp [1] analyzed the stability of two-wheeled vehicle about straight running by using the model of four degree-of-freedom. It indicated that the steering angle, the side slip of bicycle body, the angle of bicycle body, and the lean angle affect the stability of two-wheeled vehicle under the straight running. In addition, the features of two-wheeled vehicle body and tire were investigated by this model. A paper discussed by Grasser and D'Arrigo [2] proposed a novel type of two-wheeled vehicle which run by the shift of driver's weight. Two papers developed by Tanaka and Murakami [3], Niki and Murakami [4] had realized the stable running of bicycle by controlling the steering angle of handle. Recently, the stability of the bicycle at low speed is investigated by Iuchi et al. [5]. In the motion of bicycle, the center of gravity (CG) and the steering angle of handle are important to realize a stable running motion. Both these signals are elegantly finished by human on a bicycle and therefore the stable bicycle motion is achieved. This paper proposes an autonomous balance using the CG and the steering angle of handle to realize a human-like operation in an electric bicycle. Furthermore, it can expand to autonomous balance of the bicycle with variable speed.

In an electric bicycle, two strategies are taken up to stabilize the running motion of an electrical bicycle. One is the control of its center of gravity (CG), and the other is the control of its steering angle of handle. In general, a pendulum is used for the control of the CG. In addition, the bicycle often possesses a lean angle with respect to vertical direction. In this situation, the electrical bicycle has two control inputs: the control of the handle and the control of the pendulum. On the other hand, the proposed system contains three outputs: steering angle, lean angle, and pendulum angle, affecting the dynamical balance of electrical bicycle. However, the paper by Ichui et al. [5] merely uses a linearized model of an electrical bicycle to design a linear controller. Astrom et al. [6] also discuss the dynamics and control of bicycles via a linearized approach. These control methodologies only force the operating point into the vicinity of the desired posture or merely drive the operating point near desired attitude to the target. In this situation, an autonomous dynamic balance is difficult to obtain as the electrical bicycle is encountered with huge uncertainties, e.g., different ground conditions, external disturbances in the air.

A nonlinear control for an underactuated acrobot is constructed by Berkemeier and Fearing [7]. For the trajectory of 1 *Hz*, no tracking error for their controller occurs as compared with the tracking error of 13° for the pseudolinearizing controller. It reveals that the response of nonlinear dynamic system via a nonlinear controller is often much better than that via a linear controller. It is also known that variable structure control (VSC) uses discontinuous control action to drive state trajectories toward a specific hyper-plane in the state space, and to maintain the state trajectories sliding on the specific hyper-plane until the origin of the state space is reached [8-12]. This peculiar system feature is claimed to result in an excellent system performance including insensitivity to parameter variations and rejection of disturbances. Although this control methodology probably results in a chattering control input, many methods have been developed to reduce the possibility of chattering control input, e.g., forward control to attenuate the uncertainties [9], time-varying boundary layer [10], sliding sector [12]. As the authors realize, no paper has discussed the VSC with the number of output larger than that of control input. This is the so-called variable structure under-actuated control (VSUAC). The motivation of using the VSUAC for the electrical bicycle is that its uncertainties are often huge due to different ground conditions (e.g., wet ground, muddy ground, concrete ground, different tires) and a gust of wind outside of house. Merely use an ordinary proportional- derivative-integral (PID) control or other linear controls often can not have good robust performance.

II. Modeling and Problem Formulation

A. Modeling of electrical bicycle

In the beginning, the control mechanism of an electrical bicycle is depicted in Fig. 1. The corresponding parameters are given and described in Table 1. First, the following states: $x_1(t)=\theta(t)$, $x_2(t)=\phi_1(t)$, $x_3(t)=\phi_2(t)$, $x_4(t)=\dot{\theta}(t)$, $x_5(t)=\dot{\phi}_1(t)$, and $x_6(t)=\dot{\phi}_2(t)$, are defined. Then the corresponding dynamic equation in state-space form is achieved as follows:

$$\dot{x}_1(t)=x_4(t)=\bar{a}_1(x)$$
$$\dot{x}_2(t)=x_5(t)=\bar{a}_2(x)$$
$$\dot{x}_3(t)=x_6(t)=\bar{a}_3(x)$$
$$\dot{x}_4(t)=\{f\,mg\sin x_2(t)+I_w\omega\,x_5(t)$$
$$-\left(C_t x_2(t)t_r\cos x_1(t)+\mu\,\omega t_r\sin x_1(t)\right)+\tau_{han}(t)\}/I_h$$
$$=\bar{a}_4(x)+\bar{b}_{41}(x)\tau_{han}(t)$$
$$\dot{x}_5(t)=\{-\left(M_p l_2^2+M_p l_1 l_2\cos x_3(t)+J_2\right)\left(M_p l_1 l_2 x_5^2\sin x_3(t)\right)$$
$$+\left(2M_p l_1 l_2 x_5(t)x_6(t)\sin x_3(t)\right)\left(M_p l_2^2+J_2\right)$$
$$+\left(M_p l_2^2+M_p l_1 l_2\cos x_3(t)+J_2\right)\left(M_p g l_2\sin\left(x_3(t)-x_2(t)\right)\right)$$
$$+\left(M_p l_1 l_2 x_6^2(t)\sin x_3(t)\right)\left(M_p l_2^2+J_2\right)$$
$$+\left(M_p l_2^2+M_p l_1 l_2\cos x_3(t)+J_2\right)$$
$$\cdot\left[M_p l_2\cos\left(x_3(t)-x_2(t)\right)\left(\frac{V^2}{L}x_1(t)+\frac{L_1 V}{L}x_4(t)\right)\right]$$
$$+\left(M_b g h\sin x_2(t)\right)\left(M_p l_2^2+J_2\right)+\left(M_p g l_1\sin x_2(t)\right)\left(M_p l_2^2+J_2\right)$$
$$-\left(M_p g l_2\sin\left(x_3(t)-x_2(t)\right)\right)\left(M_p l_2^2+J_2\right)$$
$$-\left[M_b l_1\cos x_2(t)+M_p l_2\cos x_2(t)+M_p l_2\cos\left(x_3(t)-x_2(t)\right)\right]$$
$$\cdot\left(\frac{V^2}{L}x_1(t)+\frac{L_1 V}{L}x_4(t)\right)\left(M_p l_2^2+J_2\right)$$
$$+\left(M_p l_2^2+M_p l_1 l_2\cos x_3(t)+J_2\right)\tau_{pen}(t)\}/F(x_2,x_3)$$
$$=\bar{a}_5(x)+\bar{b}_{52}(x)\tau_{pen}(t)$$
$$\dot{x}_6(t)=\{\left(M_b h^2+M_p l_1^2+M_p l_2^2+2M_p l_1 l_2\cos x_3(t)+J_1+J_2\right)$$
$$\cdot\left(M_p l_1 l_2 x_5^2(t)\sin x_3(t)\right)$$
$$-\left(M_p l_2^2+M_p l_1 l_2\cos x_3(t)+J_2\right)\left(2M_p l_1 l_2 x_5(t)x_6(t)\sin x_3(t)\right)$$
$$-\left(M_b h^2+M_p l_1^2+M_p l_2^2+2M_p l_1 l_2\cos x_3(t)+J_1+J_2\right)$$
$$\left(M_p g l_2\sin\left(x_3(t)-x_2(t)\right)\right)$$
$$-\left(M_p l_1 l_2 x_6^2\sin x_3(t)\right)\left(M_p l_2^2+M_p l_1 l_2\cos x_3(t)+J_2\right)$$
$$-\left(M_b h^2+M_p l_1^2+M_p l_2^2+2M_p l_1 l_2\cos x_3(t)+J_1+J_2\right)$$
$$\cdot\left[M_p l_2\cos\left(x_3(t)-x_2(t)\right)\left(\frac{V^2}{L}x_1(t)+\frac{L_1 V}{L}x_4(t)\right)\right]$$
$$-\left(M_b g h\sin x_2(t)\right)\left(M_p l_2^2+M_p l_1 l_2\cos x_3(t)+J_2\right)$$
$$-\left(M_p g l_1\sin x_2(t)\right)\left(M_p l_2^2+M_p l_1 l_2\cos x_3(t)+J_2\right)$$
$$+\left(M_p g l_2\sin\left(x_3(t)-x_2(t)\right)\right)\left(M_p l_2^2+M_p l_1 l_2\cos x_3(t)+J_2\right)$$
$$+\left[M_b l_1\cos x_2(t)+M_p l_2\cos x_2(t)+M_p l_2\cos\left(x_3(t)-x_2(t)\right)\right]$$
$$\cdot\left(\frac{V^2}{L}x_1(t)+\frac{L_1 V}{L}x_4(t)\right)\left(M_p l_2^2+M_p l_1 l_2\cos x_3(t)+J_2\right)$$
$$-\left(M_b h^2+M_p l_1^2+M_p l_2^2+2M_p l_1 l_2\cos x_3(t)+J_1+J_2\right)$$
$$\tau_{pen}(t)\}/G(x_3)=\bar{a}_6(x)+\bar{b}_{62}(x)\tau_{pen}(t) \quad (1a)$$

where

$$F(x_3)=\left(M_b h^2+M_p l_1^2+M_p l_2^2+2M_p l_1 l_2\cos x_3(t)+J_1+J_2\right)$$
$$\cdot\left(M_p l_2^2+J_2\right)-\left(M_p l_2^2+M_p l_1 l_2\cos x_3(t)+J_2\right)^2 \quad (1b)$$
$$G(x_3)=-F(x_3). \quad (1c)$$

Or, the corresponding matrix form is written as follows:

$$\dot{x}(t)=\bar{a}(x)+\bar{B}(x)u(t) \quad (2)$$

where $x(t)=\left[x_1(t)\;\; x_2(t)\;\; x_3(t)\;\; x_4(t)\;\; x_5(t)\;\; x_6(t)\right]^T\in\Re^6$ denotes the available system state; $\bar{a}(x)=\left[\bar{a}_1(x)\;\; \bar{a}_2(x)\;\; \bar{a}_3(x)\;\; \bar{a}_4(x)\;\; \bar{a}_5(x)\;\; \bar{a}_6(x)\right]^T$ denotes a mapping from $\Re^6\to\Re^6$; $\bar{B}(x)=\begin{bmatrix}0&0&0&\bar{b}_{41}(x)&0&0\\0&0&0&0&\bar{b}_{52}(x)&\bar{b}_{62}(x)\end{bmatrix}^T$ denotes a mapping from $\Re^6\to\Re^{6\times 2}$; and $u(t)=\left[\tau_{han}(t)\;\; \tau_{pen}(t)\right]^T\in\Re^2$ represents the control input. It is assumed that the nominal system, i.e., $\bar{a}(x)$ and $\bar{B}(x)$, is known.

B. Problem formulation

Because the motion of an electrical bicycle is often in different operating conditions (e.g., concrete ground, muddy ground, wet ground, and a gust of wind), the dynamics of an electrical bicycle is nonlinear and time variant. Hence, it is assumed that the controlled system is in face of the nonlinear time-varying uncertainties $\Delta a(x,t)$ and $\Delta B(x,t)$. The control objective of this paper is to design the control input $u(t)$, which is based on the nominal system $\bar{a}(x)$ and $\bar{B}(x)$, such that the outputs $x_1(t)=\theta(t)$, $x_2(t)=\phi_1(t)$ and $x_3(t)=\phi_2(t)$ exponentially converge into a bounded set of zero so that the dynamic balance of the electrical bicycle is obtained (c.f. Fig. 2).

III. Controller Design

Because the proposed control is an under-actuated control system, the following two switching surfaces are first defined.

$$s_1(t)=d_{1v}\left(\dot{r}_1(t)-x_4(t)\right)+d_{1p}\left(r_1(t)-x_1(t)\right) \quad (3)$$
$$s_2(t)=d_{2v}\left(\dot{r}_3(t)-x_6(t)\right)+d_{2p}\left(r_3(t)-x_3(t)\right) \quad (4)$$

where $d_{1v},d_{1p},d_{2v},d_{2p}>0$ or <0, i.e., they are the same sign to obtain two stable switching surfaces $s_1(t)$ and $s_2(t)$, and the reference inputs $r_1(t)$ and $r_3(t)$ are assigned as follows:

$$r_1(t)=k_{1v}\left(\dot{r}_2(t)-x_5(t)\right)+k_{1p}\left(r_2(t)-x_2(t)\right) \quad (5)$$
$$r_3(t)=k_{2v}\left(\dot{r}_2(t)-x_5(t)\right)+k_{2p}\left(r_2(t)-x_2(t)\right) \quad (6)$$

where $k_{1v},k_{1p},k_{2v},k_{2p}>0$ or <0, i.e., they are the same sign to obtain two stable reference inputs $r_1(t)$ and $r_3(t)$. The reason to design the reference signals of (5) and (6) is the uncontrolled state $x_2(t)$ and $x_5(t)$ should be simultaneously included into the two control modes (i.e., $x_1(t),x_3(t)$ or $x_4(t),x_6(t)$) so that they are indirectly manipulated by the controllable states.

Based on the (5), (6) and (2),

$$\dot{r}_1(t) = k_{1v}\left(\ddot{r}_2(t) - \dot{x}_5(t)\right) + k_{1p}\left(\dot{r}_2(t) - \dot{x}_2(t)\right)$$
$$= k_{1v}\left[\ddot{r}_2(t) - \bar{a}_5(x) - \Delta a_5(x,t) - \left(\bar{b}_{52}(x) + \Delta b_{52}(x,t)\right)u_2(t)\right] \quad (7)$$
$$+ k_{1p}\left(\dot{r}_2(t) - x_5(t)\right) = \dot{\bar{r}}_1(t) + \Delta\dot{r}_1(t)$$
$$\dot{r}_3(t) = k_{2v}\left(\ddot{r}_2(t) - \dot{x}_5(t)\right) + k_{2p}\left(\dot{r}_2(t) - \dot{x}_2(t)\right)$$
$$= k_{2v}\left[\ddot{r}_2(t) - \bar{a}_5(x) - \Delta a_5(x,t) - \left(\bar{b}_{52}(x) + \Delta b_{52}(x,t)\right)u_2(t)\right] \quad (8)$$
$$+ k_{2p}\left(\dot{r}_2(t) - x_5(t)\right) = \dot{\bar{r}}_3(t) + \Delta\dot{r}_3(t)$$

where $\dot{\bar{r}}_1(t), \dot{\bar{r}}_3(t)$ and $\Delta\dot{r}_1(t)$, $\Delta\dot{r}_3$ represent the nominal and uncertain values of $\dot{r}_1(t)$ and $\dot{r}_3(t)$, respectively. That is,

$$\dot{\bar{r}}_1(t) = k_{1v}\left[\ddot{r}_2(t) - \bar{a}_5(x) - \bar{b}_{52}(x)u_2(t)\right] + k_{1p}\left(\dot{r}_2(t) - x_5(t)\right) \quad (9)$$
$$\dot{\bar{r}}_3(t) = k_{2v}\left[\ddot{r}_2(t) - \bar{a}_5(x) - \bar{b}_{52}(x)u_2(t)\right] + k_{2p}\left(\dot{r}_2(t) - x_5(t)\right) \quad (10)$$

and the remaining signals from (7) and (8) denote $\Delta\dot{r}_1(t)$ and $\Delta\dot{r}_3(t)$. Then the derivatives of two switching surfaces (3) and (4) are described as follows:

$$\dot{s}_1(t) = d_{1v}\left(\ddot{r}_1(t) - \dot{x}_4(t)\right) + d_{1p}\left(\dot{r}_1(t) - \dot{x}_1(t)\right)$$
$$= d_{1v}\left[\dddot{\bar{r}}_1(t) - \dot{\bar{a}}_4(x) - \dot{\bar{b}}_{41}(x)u_1(t)\right] + d_{1p}\left(\ddot{\bar{r}}_1(t) - x_4(t)\right) + \Delta\Omega_1(x,t) \quad (11)$$
$$\dot{s}_2(t) = d_{2v}\left(\ddot{r}_3(t) - \dot{x}_6(t)\right) + d_{2p}\left(\dot{r}_3(t) - \dot{x}_3(t)\right)$$
$$= d_{2v}\left[\dddot{\bar{r}}_3(t) - \dot{\bar{a}}_6(x) - \dot{\bar{b}}_{62}(x)u_2(t)\right] + d_{2p}\left(\ddot{\bar{r}}_6(t) - x_6(t)\right) + \Delta\Omega_2(x,t) \quad (12)$$

where $\Delta\Omega_1(x,t)$ and $\Delta\Omega_2(x,t)$ are uncertain signals described as follows:

$$\Delta\Omega_1(x,t) = d_{1v}\left[\Delta\dddot{r}_1(t) - \Delta\dot{a}_4(x,t) - \Delta\dot{b}_{41}(x,t)u_1(t)\right] + d_{1p}\Delta\ddot{r}_1(t) \quad (13)$$
$$\Delta\Omega_2(x,t) = d_{2v}\left[\Delta\dddot{r}_3(t) - \Delta\dot{a}_6(x,t) - \Delta\dot{b}_{62}(x,t)u_2(t)\right] + d_{2p}\Delta\ddot{r}_3(t). \quad (14)$$

The proposed VSUAC contains an equivalent control (15), i.e., $u_{1eq}(t)$ and $u_{2eq}(t)$, to deal with a nominal system, and a switching control (16), i.e., $u_{1sw}(t)$ and $u_{2sw}(t)$, to cope with the uncertainties.

$$u_{1eq}(t) = \left\{d_{1v}\left(\dddot{\bar{r}}_1(t) - \dot{\bar{a}}_4(x)\right) + d_{1p}\left(\ddot{\bar{r}}_1(t) - x_4(t)\right)\right\}/\left[d_{1v}\bar{b}_{41}(x)\right] \quad (15a)$$
$$u_{2eq}(t) = \left\{d_{2v}\left(\dddot{\bar{r}}_3(t) - \dot{\bar{a}}_6(x)\right) + d_{2p}\left(\ddot{\bar{r}}_3(t) - x_6(t)\right)\right\}/\left[d_{2v}\bar{b}_{62}(x)\right] \quad (15b)$$
$$u_{1sw}(t) = \left\{\eta_{11}s_1(t) + \eta_{12}s_1(t)/\left[\left|s_1(t)\right| + \varepsilon_1\right]\right\}/\left[(1-\lambda_1)d_{1v}\bar{b}_{41}(x)\right] \quad (16a)$$
$$u_{2sw}(t) = \left\{\eta_{21}s_2(t) + \eta_{22}s_2(t)/\left[\left|s_2(t)\right| + \varepsilon_2\right]\right\}/\left[(1-\lambda_2)d_{2v}\bar{b}_{62}(x)\right] \quad (16b)$$

where $d_{1v}\bar{b}_{41}(x)$ and $d_{2v}\bar{b}_{62}(x)$ are nonsingular for all $x(t)$, $\eta_{ij} > 0, i, j = 1,2$, are the switching gains, $\varepsilon_1, \varepsilon_2 \geq 0$, are the boundary layer, and λ_1, λ_2 denote the upper bound of the uncertain control gains and satisfy the following inequalities:

$$\left|d_{1v}\Delta b_{41}(x,t)/\left(d_{1v}\bar{b}_{41}(x)\right)\right| \leq \lambda_1 < 1, \ \forall x(t), t \quad (17a)$$
$$\left|d_{2v}\Delta b_{62}(x,t)/\left(d_{2v}\bar{b}_{62}(x)\right)\right| \leq \lambda_2 < 1, \ \forall x(t), t. \quad (17b)$$

Using (11), (12) and (15), the derivative of the switching surface is then described as follows:

$$\dot{s}_1(t) = -\left[\left(d_{1v}\bar{b}_{41}(x)\right) + d_{1v}\Delta b_{41}(x,t)\right]u_{1sw}(t) + \Delta\Omega_1'(x,t) \quad (18a)$$
$$\dot{s}_2(t) = -\left[\left(d_{2v}\bar{b}_{62}(x)\right) + d_{2v}\Delta b_{62}(x,t)\right]u_{2sw}(t) + \Delta\Omega_2'(x,t) \quad (18b)$$

where

$$\Delta\Omega_1'(x,t) = d_{1v}\left[\Delta\dddot{r}_1(t) - \Delta\dot{a}_4(x,t) - \Delta\dot{b}_{41}(x,t)u_{1eq}(t)\right] + d_{1p}\Delta\ddot{r}_1(t) \quad (19a)$$
$$\Delta\Omega_2'(x,t) = d_{2v}\left[\Delta\dddot{r}_3(t) - \Delta\dot{a}_6(x,t) - \Delta\dot{b}_{62}(x,t)u_{2eq}(t)\right] + d_{2p}\Delta\ddot{r}_3(t) \quad (19b)$$

and their upper bounds are estimated as follows:

$$\left|\Delta\Omega_1'(x,t)\right| \leq h_1(x) + \mu_1, \ \left|\Delta\Omega_2'(x,t)\right| \leq h_2(x) + \mu_2 \quad (20)$$

where $h_1(x), h_2(x), \mu_1$ and $\mu_2 > 0$, and theses are all known. Then the following theorem discussing the control of the electrical bicycle using the VSUAC is given.

Theorem 1: Consider the electrical bicycle (2) and the VSUAC (15) and (16) with $\eta_{11}, \eta_{21} > \delta/2 > 0$, $\eta_{12} > h_1(x) + \mu_1$, and $\eta_{22} > h_2(x) + \mu_2$. Together with the conditions (17) and (20), $s_1(t), s_2(t), u_1(t)$ and $u_2(t)$ are ultimately uniformly bounded (UUB) and the tracking performance is achieved as follows:

$$D = \left\{s_1(t), s_2(t) \in \Re \middle| 0 \leq \left|s_1(t)\right| \leq p_{\max}, \left|s_2(t)\right| \leq q_{\max}\right\} \quad (21)$$

where

$$p_{\max} = \max_x\left[p(x)\right], q_{\max} = \max_x\left[q(x)\right] \quad (22)$$
$$p(x) = \sqrt{p_1^2(x) + p_2(x)} - p_1(x),$$
$$q(x) = \sqrt{q_1^2(x) + q_2(x)} - q_1(x) \quad (23)$$
$$p_1(x) = \left\{\varepsilon_1 + \left[\eta_{12} - h_1(x) - \mu_1\right]/\left(\eta_{11} - \delta/2\right)\right\}/2,$$
$$q_1(x) = \left\{\varepsilon_2 + \left[\eta_{22} - h_2(x) - \mu_2\right]/\left(\eta_{21} - \delta/2\right)\right\}/2 \quad (24)$$

and

$$p_2(x) = \varepsilon_1\left(h_1(x) + \mu_1\right)/\left(\eta_{11} - \delta/2\right),$$
$$q_2(x) = \varepsilon_2\left(h_2(x) + \mu_2\right)/\left(\eta_{21} - \delta/2\right). \quad (25)$$

Proof: See *Appendix A*.

Remark 1: The assumptions of Theorem 1 are explained as follows: (1) Conditions (17a) and (17b) denote the uncertainty of control gain as compared with its nominal value. It indicates that this uncertainty must be smaller than the corresponding nominal value. (ii)Conditions (20) denoting the upper bound of the uncertainty must be known. Its upper bound is connected with system performance. From (21)-(25), the larger $h_1(x)$ or μ_1 or $h_2(x)$ or μ_2, the larger $\left|s_1(t)\right|$ or $\left|s_2(t)\right|$.

IV. Simulations and Discussions

Consider the electrical bicycle (2) as shown in Table 1. The corresponding sinusoidal responses for some representative amplitudes and frequencies are shown in the Fig. 3, which indicates that the dynamics of electrical bicycle is highly nonlinear and unstable [1-7]. The ordinary PID control can not stabilize the electrical bicycle. For brevity, those are omitted. However, it can be stabilized by the following modified proportional- derivative control (MPDC) (see e.g., [5]):

$$u_{1mpd}(t) = d_{1v}\left(\dot{\bar{r}}_1(t) - x_4(t)\right) + d_{1p}\left(r_1(t) - x_1(t)\right) \quad (26a)$$
$$u_{2mpd}(t) = d_{2v}\left(\dot{\bar{r}}_3(t) - x_6(t)\right) + d_{2p}\left(r_3(t) - x_3(t)\right) \quad (26b)$$

where $r_1(t), \dot{\bar{r}}_1(t), r_3(t)$ and $\dot{\bar{r}}_3(t)$ are respectively obtained from (5),(6), (9) and (10) with these parameters $k_{1v} = 1.0, k_{1p} = 10$, $k_{2v} = 0.5$ and $k_{2p} = 17$. In this paper, the reference input of the lean angle and velocity and the reference inputs of the nominal steering acceleration and pendulum acceleration are set zero, i.e., $r_2(t) = 0$, $\dot{r}_2(t) = 0$, $\ddot{\bar{r}}_1(t) = 0$, and $\ddot{\bar{r}}_3(t) = 0$. The uncertainty for the system (2) with the multiplication form (i.e.,

$\bar{a}_i(x)(1+\Delta a_i(x,t))$, $i=4,5,6$ $\bar{b}_{41}(x)(1+\Delta b_{41}(x,t))$, $\bar{b}_{52}(x)(1+\Delta b_{52}(x,t))$, and $\bar{b}_{62}(x)(1+\Delta b_{62}(x,t))$ is assumed to be:

$$\begin{aligned}
&\Delta a_4(x,t) = 1.5x_1(t)x_2(t)\sin(0.3t\,x_5(t)) \\
&-0.37x_3(t)x_6(t)\cos(0.2tx_6(t)) - 0.2\sin(100t) \\
&\Delta a_5(x,t) = 1.5x_2(t)x_3(t)\sin(0.3t\,x_6(t)) \\
&-0.37x_1(t)x_4(t)\cos(0.1tx_5(t)) - 0.2\cos(200t) \\
&\Delta a_6(x,t) = 1.5x_3(t)x_1(t)\sin(0.3t\,x_4(t)) \\
&+0.37x_2(t)x_5(t)\cos(0.3t\,x_4(t)) + 0.2\sin(300t) \\
&\Delta b_{41}(x,t) = 0.3\sin(-0.1+9.6t\,x_3(t)) + 0.5\sin(300t) \\
&\Delta b_{52}(x,t) = 0.3\sin(-0.1+10.7t\,x_2(t)) + 0.5\sin(200t) \\
&\Delta b_{62}(x,t) = 0.3\sin(0.1+6.9t\,x_1(t)) - 0.5\cos(100t).
\end{aligned} \tag{27}$$

The following simulations use the numerical algorithm of fourth-order Runge-Kutta with time step 0.01 second. For example, the acceptable response of the electrical bicycle in the presence of the uncertainty (27) by the MPDC with $d_{1v}=6.58$, $d_{1p}=31.5$, $d_{2v}=2.7$ and $d_{2p}=10.5$ is presented in Fig. 4. The responses of other suitable parameters are similar with Fig. 4. For simplicity, those are omitted. For comparison between the MPDC and the proposed VSUAC, the coefficients of two switching surfaces are the same as the parameters of the MPDC. The control parameters of the VSUAC are set as follows: $\eta_{11}=20, \eta_{12}=1.5$, $\eta_{21}=12, \eta_{22}=6$, $\varepsilon_1=\varepsilon_2=0.1$, and $\lambda_1=\lambda_2=0.5$. The response for the electrical bicycle in the presence of the uncertainty (27) by the VSUAC is shown in Fig. 5. It indicates that the performance of the MPDC (i.e., Fig.4) is improved by the proposed VSUAC. For the consideration of practical situations (e.g., a gust of wind is blown to the bicycle), the following simulation with the uncertainty (27) and pulse disturbance is investigated. It is assumed that a gust of wind during the period 4.0~4.1 second brings about the extra effect of the lean angle 5° between 4 and 4.1 second. The corresponding result by the VSUAC is shown in Fig. 6. For comparison with the result of the MPDC, its corresponding response is then presented in Fig. 7. From these two figures, we know the resistance of the pulse disturbance by the VSUAC is superior to that of the MPDC. From practical viewpoint, the following simulation with the saturation $|\tau_{han}(t)|, |\tau_{pen}(t)| < \tau_{\max}$, where $\tau_{\max}=15Nm$, is shown in Fig. 8. From Fig.8, we know that the saturation of the control input does not necessarily result in a worse performance. As one knows, the bicycle can be manipulated in a variable speed. Hence, the corresponding result is examined by the Fig. 9 for $V(t)=3+3\sin(0.2\pi)m/s$. It reveals that the proposed control can deal with a variable speed with 0.1 Hz from 0 to $6\,m/s$. The response by the proposed control is acceptable (cf. Fig. 9(a)); however, the corresponding result by the MPDC is unstable (cf. Fig. 9(b)). Finally, an implementation of the electrical bicycle is applied by an embedded control system, e.g., TMS320F2812 from TI Co. Is the control cycle time can be larger than the 10*ms* of the above setting? Based on this requirement, the corresponding results of Fig. 5 using the control cycle time 100 and 50*ms* are investigated. The response using the control cycle time 100*ms* is unstable for the original setting. The response using the control cycle time 50*ms* becomes sluggish. For simplicity, these are omitted. Based on the above-mentioned investigations, the important observations are depicted as follows: (i) The dynamics of an electrical bicycle is nonlinear, complex, time-variant, and unstable. (ii)The VSUAC can improve the performances of the MPDC and ordinary PID control.(iii) Not too large saturated control input for the VSUAC does not necessarily result in a worse performance. (iv)The control cycle time of the electrical bicycle must be small enough. In our case, the control cycle time larger than 100*ms* will result in an inability. (v) The resistance of the pulse disturbance (e.g., a gust of wind) by the VSUAC is much better than that of the MPDC. (vi)The proposed VSUAC can be applied to the bicycle having variable speed with 0.1 Hz from 0 to $6\,m/s$. However, it can not be stabilized by the MPDC.

V. Concluding Remarks

The proposed VSUAC is designed based on the original nonlinear dynamic equation. In this situation, the motion of an electrical bicycle is not limited to the neighborhood of equilibrium point. In short, the operating region of electrical bicycle by the proposed control is larger as compared with a linear controller. For example, the proposed controller is applicable to a variable speed motion of an electrical bicycle without causing instability. On the contrary, it can not be stabilized by a linear controller (see Fig. 9). The parameters of the proposed control are not critical to choose. However, suitable selection of control parameters can obtain an excellent performance. The stability of the closed-loop system is also verified by Lyapunov stability theory. The system performances, including the tracking performance for nonlinear time-varying uncertainty, the pulse disturbance for simulating the wind effect, the variable speed motion of bicycle, the saturated control input due to the limitation of signal, are improved as compared with ordinary PID control and the MPDC. Our future work is to implement this study.

References

[1] R. S. Sharp, "The stability and control of motorcycles," *Journal Mechanical Engineering Science*, vol.13, no.5, pp.316-329, 1971.

[2] F. Grasser, A. D'Arrigo, S. Colombi, and A. Rufer, "JOE: A mobile, inverted pendulum," *IEEE Trans. Ind. Electron.,* vol. 49, no. 1, pp. 107-114, Feb. 2002.

[3] Y. Tanaka and T. Murakami, "Self sustaining bicycle robot with steering controller," *IEEE 8th International Workshop on Advanced Motion Control*, pp. 193 -197, March 25th -28th, 2004.

[4] H. Niki and T. Murakami, "An approach to self stabilization of bicycle motion by handle controller" *IEEE Trans. Ind. Applica.*, vol.125, no. 8, pp. 779-785, 2005.

[5] K. Iuchi, H. Niki and T. Murakami, "Attitude control of bicycle motion by steering angle and variable COG control," *32nd Annual Conference of IEEE IECON,* pp. 2065-2070, Nov.2005.

[6] K. J. Astrom, R. E. Klein and A Lennartsson, "Bicycles dynamics and control," *IEEE Contr. Syst. Magazine*, vol.

25, no. 4, pp.26-47, Aug. 2005.
[7] M. D. Berkemeier and R. S. Fearing, "Tracking fast inverted trajectories of the underactuated acrobot," *IEEE Trans. Robotics & Autom.*, vol. 15, no. 4, pp. 740-759, 1999.
[8] Y. Hung, W. Gao and J. C. Hung, "Variable structure control: A survey," *IEEE Trans. Ind. Electron.*, vol. 40, no. 1, pp. 2-22, 1993.
[9] C. L. Hwang and J. C. Hsu, "Nonlinear control design for a Hammerstein model system," *IEE Proceedings-D, Control Theory and Application,* vol. 142, no. 4, pp. 277-285, 1995.
[10] C. L. Hwang, " Sliding mode control using time-varying switching gain and boundary layer for electrohydraulic position and differential pressure control," *IEE Proceedings-D, Control Theory and Application*, vol. 143, no. 4, pp. 325-332, 1996.
[11] K. D. Young, V. I. Utkin and Ümit Özgüner, "A control Engineer's guide to sliding mode control," *IEEE Trans. Contr. Syst. Technol.*, vol. 7, no. 3, pp. 328-342, 1999.
[12] Furuta, K. and Pan, Y. , "Variable structure control with sliding sector", *IFAC J. of Automatica*, vol. 36, no. 2, pp. 211-228, 2000.

Appendixes

Appendix A (*The proof of Theorem 1*):

For simplicity, the arguments of variable are omitted. Define the following Lyapunov function:

$$V = \left(s_1^2 + s_2^2\right)/2 > 0, \text{as } s_1 \neq 0 \text{ or } s_2 \neq 0. \quad \text{(B1)}$$

Taking the time derivative of (B1) and assuming that $\dot{V} \leq -\delta V$, where $\delta > 0$, gives

$$\dot{\bar{V}} = s_1\dot{s}_1 + s_2\dot{s}_2 + \delta\left(s_1^2 + s_2^2\right)/2 \quad \text{(B2)}$$

where $\dot{\bar{V}} = \dot{V} + \delta V$. Substituting (16), (18), and (20) into (B2) yields

$$\dot{\bar{V}} = s_1\left\{-\frac{\left(1+d_{1v}\Delta b_{41}/d_{1v}\bar{b}_{41}\right)}{1-\lambda_1}\left(\eta_{11}s_1 + \frac{\eta_{12}s_1}{|s_1|+\varepsilon_1}\right) + \Delta\Omega_1' + \frac{\delta s_1}{2}\right\}$$

$$+ s_2\left\{-\frac{\left(1+d_{2v}\Delta b_{62}/d_{1v}\bar{b}_{62}\right)}{1-\lambda_1}\left(\eta_{21}s_2 + \frac{\eta_{22}s_2}{|s_2|+\varepsilon_2}\right) + \Delta\Omega_2' + \frac{\delta s_2}{2}\right\}$$

$$\leq -\frac{(\eta_{11}-\delta/2)|s_1|}{|s_1|+\varepsilon_1}\left\{|s_1|\left(|s_1|+\varepsilon_1\right) + \frac{\eta_{12}}{(\eta_{11}-\delta/2)}|s_1| - \frac{h_1+\mu_1}{(\eta_{11}-\delta/2)}\left(|s_1|+\varepsilon_1\right)\right\}$$

$$-\frac{(\eta_{21}-\delta/2)|s_2|}{|s_2|+\varepsilon_2}\left\{|s_2|\left(|s_2|+\varepsilon_2\right) + \frac{\eta_{22}}{(\eta_{21}-\delta/2)}|s_2| - \frac{h_2+\mu_2}{(\eta_{21}-\delta/2)}\left(|s_2|+\varepsilon_2\right)\right\}$$

$$\leq -(\eta_{11}-\delta/2)|s_1|P(|s_1|)/(|s_1|+\varepsilon_1) - (\eta_{21}-\delta/2)|s_2|Q(|s_2|)/(|s_2|+\varepsilon_2)$$

where $P(|s_1|) = |s_1|^2 + 2p_1|s_1| - p_2$ and $Q(|s_2|) = |s_2|^2 + 2q_1|s_2| - q_2$. As $|s_1| \geq p_{\max}$ and $|s_2| \geq q_{\max}$, the inequalities $P(|s_1|) \geq 0$ and $Q(|s_2|) \geq 0$ are satisfied. Then, outside of the domain D in (21) making $\dot{\bar{V}} \leq 0$ (or $\dot{V} \leq -\delta V$) is achieved. Hence, the signals s_1 and s_2 exponentially converge into the domain D. Finally, from (15) and (16) u_1 and u_2 are UUB.

Q.E.D.

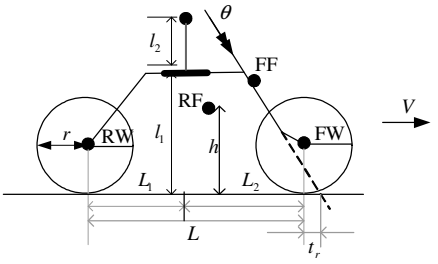

(a) Side view.

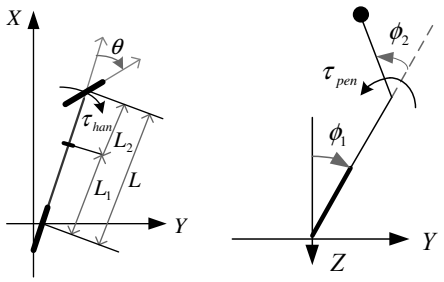

(b) Top view. (c) Rear view.

Fig. 1. Control mechanism of an electrical bicycle, where θ, ϕ_1 and ϕ_2 denote the steering, lean, and pendulum angles, respectively; τ_{han} and τ_{pen} represent the handling and pendulum torques, respectively.

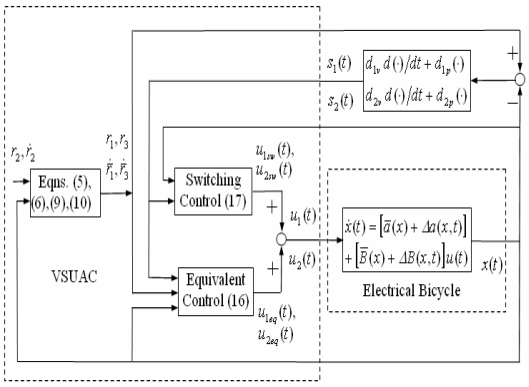

Fig. 2. Control block diagram of the overall system.

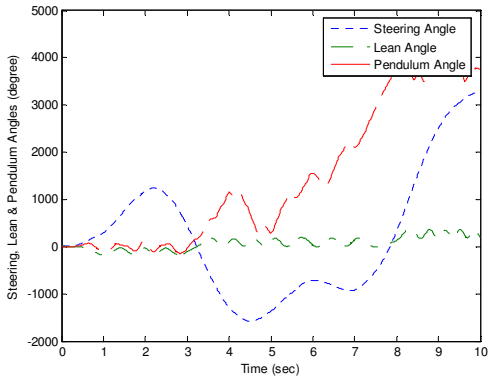

(a) $\tau_{han}(t) = 10\sin(0.6\pi)$ and $\tau_{pen}(t) = 5\sin(0.6\pi)Nm$.

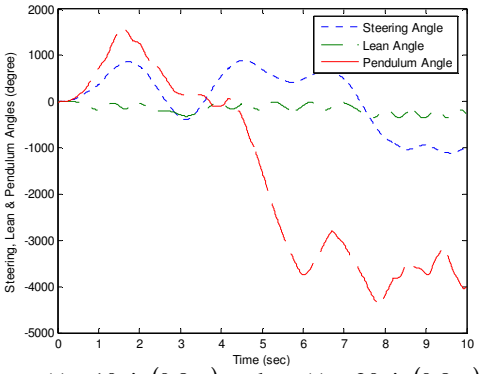

(b) $\tau_{han}(t) = 10\sin(0.8\pi t)$ and $\tau_{pen}(t) = 20\sin(0.8\pi t) Nm$.

Fig. 3. The sinusoidal responses of the electrical bicycle.

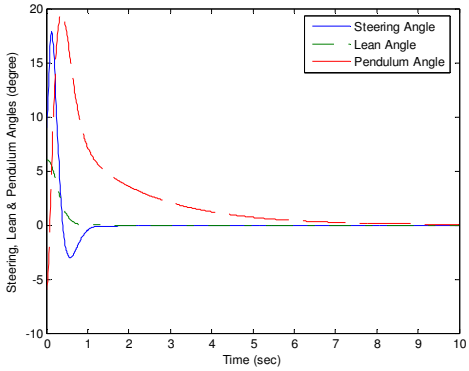

(a) System outputs $\theta(t), \phi_1(t)$ and $\phi_2(t)$.

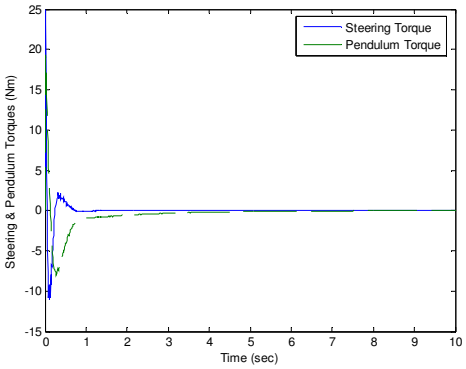

(b)Control inputs $\tau_{han}(t)$ and $\tau_{pen}(t)$.

Fig. 4. The responses of the electrical bicycle with uncertainty (27) by the MPDC.

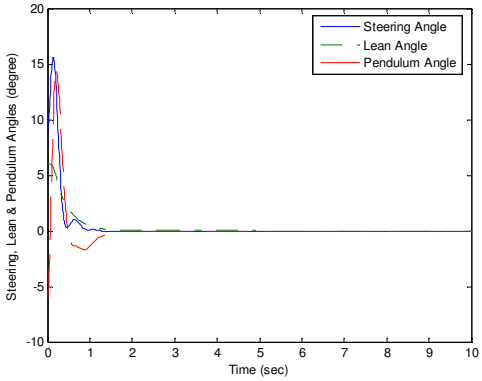

(a) System outputs $\theta(t), \phi_1(t)$ and $\phi_2(t)$.

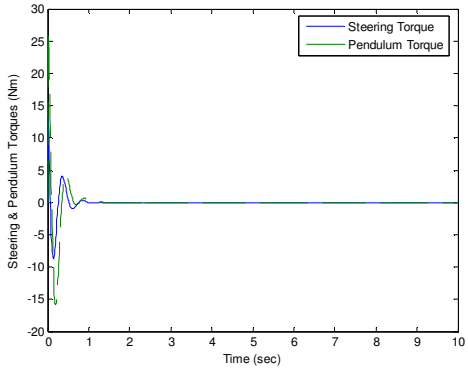

(b) Control inputs $\tau_{han}(t)$ and $\tau_{pen}(t)$.

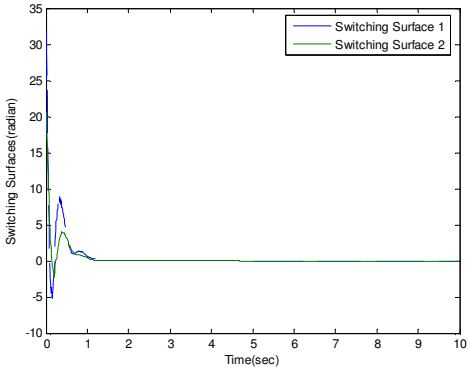

(c) Switching surfaces $s_1(t)$ and $s_2(t)$.

Fig. 5. The responses of the electrical bicycle with uncertainty (27) by the VSUAC.

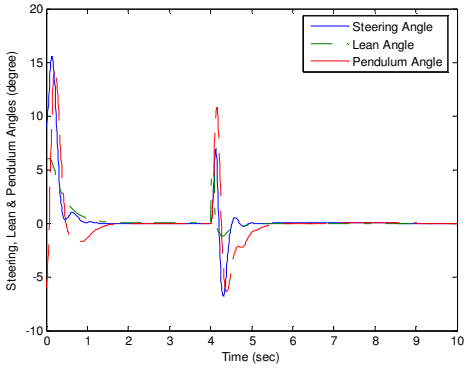

(a) System outputs $\theta(t), \phi_1(t)$ and $\phi_2(t)$.

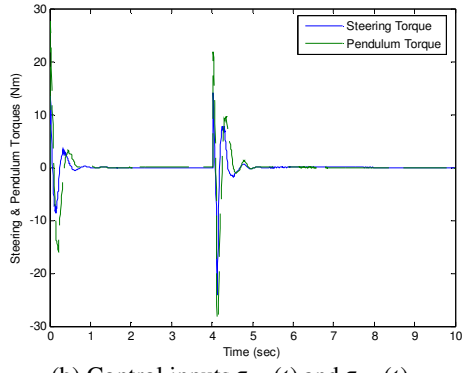

(b) Control inputs $\tau_{han}(t)$ and $\tau_{pen}(t)$.

Fig. 6. The responses of Fig. 5 in the face of the pulse disturbance of the lean angle during 4 ~4.1 second.

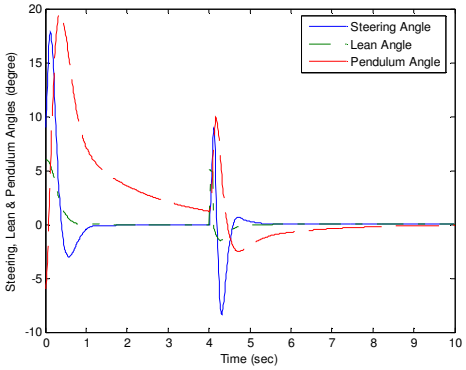

(a) System outputs $\theta(t), \phi_1(t)$ and $\phi_2(t)$.

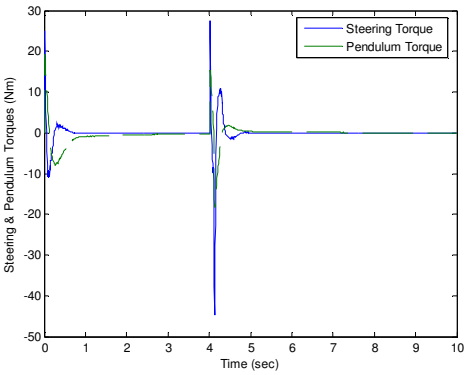

(b) Control inputs $\tau_{han}(t)$ and $\tau_{pen}(t)$.

Fig. 7. The responses of Fig. 4 in the face of the pulse disturbance at lean angle during 4 ~4.1 second.

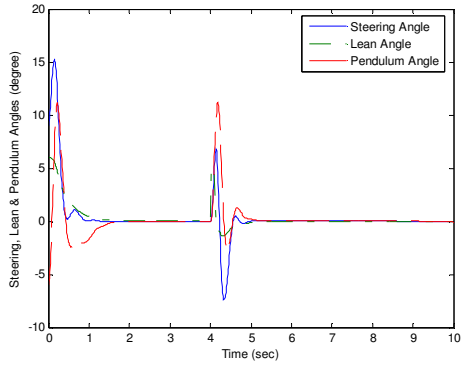

(a) System outputs $\theta(t), \phi_1(t)$ and $\phi_2(t)$.

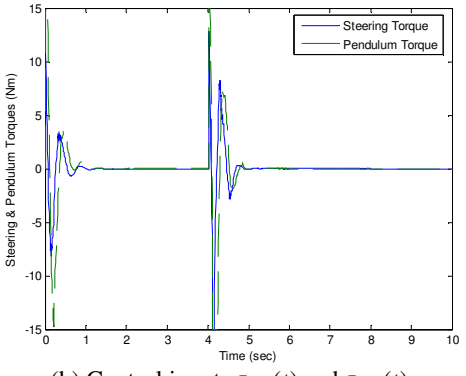

(b) Control inputs $\tau_{han}(t)$ and $\tau_{pen}(t)$.

Fig. 8. The responses of Fig. 6 with saturated control input.

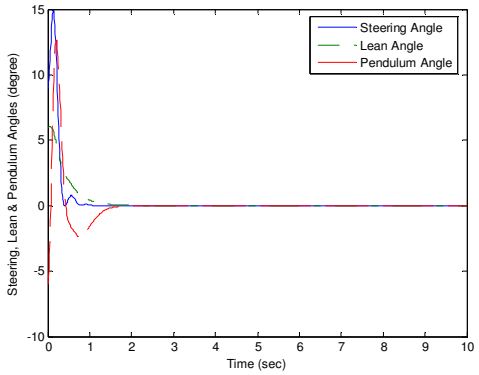

(a) VSUAC.

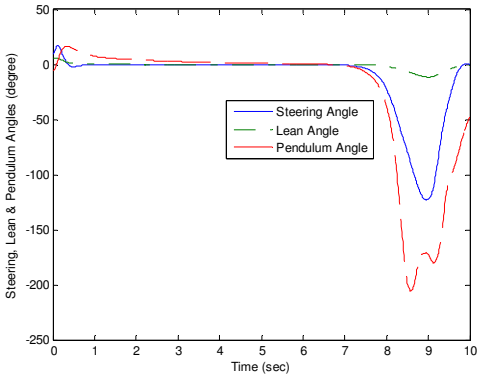

(b)MPDC.

Fig. 9. The output responses of the electrical bicycle with variable speed $V(t) = 3 + 3\sin(0.2\pi t)$ in the presence of the uncertainty (27) by the VSUAC and MPDC.

Table 1. Parameters of electrical bicycle.

Parameters	Description	Values
M_b	Mass of electrical bicycle	$52\,kg$
m	Mass of front wheel part	$10\,kg$
M_p	Mass of inverted pendulum	$2\,kg$
L	Wheel base	$1.13\,m$
L_1	CG position from rear wheel	$0.324\,m$
L_2	CG position from front wheel	$0.806\,m$
h	Height of CG	$0.855\,m$
l_1	Height of the axis of pendulum	$1\,m$
l_2	Length of pendulum	$0.51\,m$
r	Radius of wheel	$0.35\,m$
V	Velocity of bicycle	$3.0\,m/s$
f	Offset	$0.06\,m$
t_r	Trail	$0.05\,m$
l_h	Inertial of front wheel about handle axis	$0.35\,kgm^2$
I_w	Inertial of wheel	$0.18\,m$
μ	Coefficient of conflict	0.1
J_1	Inertial of CG about x axis	$10\,kgm^2$
J_2	Inertial of inverted pendulum	$0.0463\,kgm^2$
C_t	Coefficient of camber thrust	$66\,N/rad$